

Structural, magnetic and thermal properties of the substitution series $\text{Ce}_2(\text{Pd}_{1-x}\text{Ni}_x)_2\text{Sn}$

J.G. Sereni ^{1*}, G. Schmerber ², A. Braghta ³, B. Chevalier ⁴ and J.P. Kappler ²

¹ *División Bajas Temperaturas (CAB - CNEA), Conicet, 8400 S.C. Bariloche, Argentina*

² *IPCMS, UMR 7504 CNRS-ULP, 23 rue de Loess, B.P. 43 Strasbourg Cedex 2, France*

³ *Dpartement de Physique, Université de Guelma, 24000 Guelma, Algeria*

⁴ *CNRS, Université de Bordeaux, ICMCB, 87 av. Dr. Schweitzer, 33608 Pessac Cedex, France*

(Dated: March 27, 2022)

Structural, magnetization and heat capacity studies were performed on $\text{Ce}_2(\text{Pd}_{1-x}\text{Ni}_x)_2\text{Sn}$ ($0 \leq x \leq 1$) alloys. The substitution of Pd atoms by isoelectronic Ni leads to a change in the crystallographic structure from tetragonal (for $x \leq 0.3$) to centered orthorhombic lattice (for $x \geq 0.4$). The volume contraction thorough the series is comparable to the expected from the atomic size ratio between transition metal components. The consequent weak increase of the Kondo temperature drives the two transitions observed in $\text{Ce}_2\text{Pd}_2\text{Sn}$ to merge at $x = 0.25$. After about a 1% of volume collapse at the structural modification, the system behaves as a weakly magnetic heavy fermion with an enhanced degenerate ground state. Notably, an incipient magnetic transition arises on the Ni-rich side. This unexpected behavior is discussed in terms of an enhancement of the density of states driven by the increase of the $4f$ -conduction band hybridization and the incipient contribution of the first excited crystal field doublet on the ground state properties.

* E-mail-address of corresponding author: jsereni@cab.cnea.gov.ar

PACS numbers: 75.20.Hr, 71.27.+a, 75.30.Kz, 75.10.-b

I. INTRODUCTION

The large family of Rare Earth based ternary compounds with the formula $\text{R}_2\text{T}_2\text{X}$ (where $\text{R}=\text{Ln}$ [1, 2] and Ac [3], $\text{T}=\text{Transition Metals of the VIII group}$ [1, 4, 5] and $\text{X}=\text{early } p\text{-metals}$ [4]) have been investigated over the past two decades because of the variety of their magnetic behaviors. Their tetragonal Mo_2FeB_2 -type structure [6] is strongly anisotropic and can be described as successive ‘ $\text{T}+\text{X}$ ’ (at $z=0$) and ‘ R ’ (at $z=1/2$) layers. Within the Ln series, Ce and Yb elements have shown some outstanding features like double magnetic transitions in $\text{Ce}_2\text{Pd}_2\text{Sn}$ [7], reentrance of magnetic order in the $\text{Yb}_2\text{Pd}_2(\text{In},\text{Sn})$ system [8] and under applied pressure [9], a gap in the solid solution in $\text{Ce}_{2\pm x}\text{Pd}_{2\pm y}\text{In}_{1\pm z}$ alloys [2] with ferromagnetic FM and antiferromagnetic AF behaviors in the respective Ce-rich and Pd-rich branches. In the case of $\text{Yb}_2\text{Pt}_2\text{Pb}$ [10] and $\text{Ce}_2\text{Pd}_2\text{Sn}$ [11], the formation of Shastry-Sutherland lattices [12, 13] were reported as the result of geometrical frustration constrains originated in a triangular network of magnetic atoms. In the latter compound, which shows two magnetic transitions, the Shastry-Sutherland lattice formed at $T_N = 4.7\text{ K}$ is overcome by a FM ground state GS at $T_C = 3.0\text{ K}$ in a first order transition [13]. Further studies under applied magnetic field demonstrated that such an exotic phase can be suppressed by the application of a moderate magnetic field $H_{cr} = 0.11\text{ T}$ [14]

It is well known that the magnetic behavior of most of Ce-based compounds which adopt magnetic GS is governed by a competition between Kondo and Ruderman-Kittel-Kasuya-Yosida RKKY magnetic interactions. Since the Kondo effect is due to the local screening of $4f$ moments by conduction-electron spins through an AF coupling exchange parameter J_{ex} and RKKY also depends on that coupling parameter for polarizing the conduction spins, both mechanisms are basically driven by the same parameter. Experimentally, J_{ex} can be tuned by two control parameters: pressure and chemical potential variation.

Since the experimental results confirm $\text{Ce}_2\text{Pd}_2\text{Sn}$ as one of the scarce examples of FM-GS among Ce intermetallics, with stable magnetic moments and a weak Kondo effect, to drive the magnetic transition by increasing the hybridization effect (i.e. increasing the J_{ex} strength) can provide valuable information concerning the stability of the mentioned Shastry-Sutherland intermediate phase. Structural pressure, produced by the substitution of larger size Pd by smaller Ni atoms, is one of the experimental possibilities as already proved in the study of $\text{CePd}_{1-x}\text{Ni}_x$ binary alloys [15].

In the case of $\text{Ce}_2(\text{Pd}_{1-x}\text{Ni}_x)_2\text{Sn}$ alloys, it is known that the isotypic $\text{Ce}_2\text{Ni}_2\text{Sn}$ compound forms with a centered orthorhombic structure of W_2CoB_2 type [16], which behaves as a magnetically ordered Kondo system [17]. However, to our knowledge no detailed study of the structural tran-

sition and its consequence on the low temperature magnetic properties was carried up to now like in $\text{Ce}_2(\text{Pd}_{1-x}\text{Ni}_x)_2\text{In}$ [18]

In this work we present the results obtained from the study of the magnetic properties of the $\text{Ce}_2(\text{Pd}_{1-x}\text{Ni}_x)_2\text{Sn}$ alloys in order to establish the range of stability of both Mo_2FeB_2 and W_2CoB_2 -type structures under the effect of structural pressure provided by the substitution of Pd atoms by smaller isoelectronic Ni ones.

II. EXPERIMENTAL DETAILS

Polycrystalline $\text{Ce}_2(\text{Pd}_{1-x}\text{Ni}_x)_2\text{Sn}$ and La isotopic samples were prepared by conventional tri-arc melting of appropriate amounts of 99.99% Ce, La, Pd and Sn, and 99.999% pure Ni, under flowing purified argon atmosphere on a water-cooled copper hearth. The buttons were remelted several times to ensure good homogeneity. The weight losses after arc melting were less than 0.2 wt.% of total mass (each sample of a total amount of ca. 1g). Each alloy was wrapped in Ta-foil, sealed in high evacuated silica tube and heat-treated for 3 weeks at 750°C. This annealing leads to the disappearance of some extra peaks and less unfolding. The alloys show a metallic-gray lustre and were air sensitive and pyrophoric. The crystallographic structure of the annealed alloys were collected at room temperature employing a Bruker AXS D8 Advance X-ray diffractometer with monochromatic $\text{CuK}_{\alpha 1}$ radiation, within $15^\circ < 2\theta < 80^\circ$, and settings of 55 kV and 25 mA. The system was equipped with a Sol'X detector. The surface of the samples were mechanically cleaned by scraping slightly with a diamond file in a gloved box under argon gas flow. After this cleaning procedure the samples were crushed slowly under C_6H_{12} with average grain size $\leq 5\mu\text{m}$. The peak positions and major peak intensities are all consistent with those expected for materials in the Mo_2FeB_2 -type tetragonal structure for $x < 0.3$ and the W_2CoB_2 orthorhombic structure for $x > 0.4$.

The susceptibility and magnetization measurements were performed using a Superconducting Quantum Interference Device (SQUID) magnetometer running between 1.8 K and room temperature, and with applied magnetic fields up to 5T. Specific heat was measured between 1.5 and 40 K using a standard heat pulse method with $\Delta T/T \approx 1\%$.

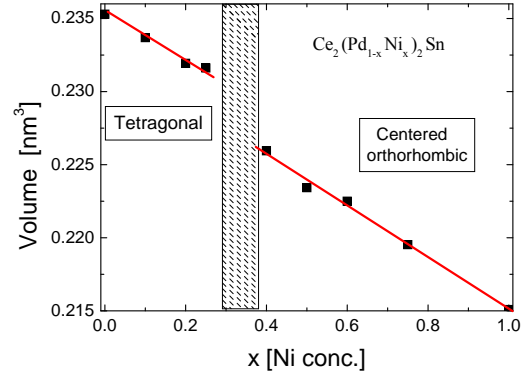


FIG. 1: (Color online) Unit cell volume dependence on Ni content, showing a discontinuity at the change of structure.

III. EXPERIMENTAL RESULTS

A. Crystalline structure

Despite of their different crystalline structures, $\text{Ce}_2\text{Pd}_2\text{Sn}$ and $\text{Ce}_2\text{Ni}_2\text{Sn}$ practically form a continuous solid solution. These stannide alloys crystallize in tetragonal Mo_2FeB_2 -type structure for $x < 0.3$ and orthorhombic W_2CoB_2 -type for $x > 0.4$, with a small gap between $0.3 < x < 0.4$. The substitution of Ni by Pd in $\text{Ce}_2(\text{Pd}_{1-x}\text{Ni}_x)_2\text{Sn}$ produces an overall volume contraction of about 8.6%, including the volume collapse of about 1% at the crystallographic transition between both structures (see Fig. 1). Such a volume reduction between both stoichiometric extremes is comparable to the contraction evaluated taking into account the relative atomic volume V difference between Pd and Ni, i.e. $100 \cdot (V_{\text{Pd}} - V_{\text{Ni}})/V_{\text{Pd}} \approx 26\%$.

On the Pd side (Mo_2FeB_2 -type structure) the volume variation stems from the change of the two lattice parameters (c.f. a and c), with the consequent variation of the Ce-Ce spacing. On the Ni-rich side, the Ce-Ce spacing decreases due to a $\approx 4\%$ decrease of a (from 0.4562 nm to 0.4381 nm) and $\approx 2\%$ b (from 0.5829 nm to 0.5728 nm), whereas the c parameter even increases by $\approx 1\%$ (from 0.8496 nm to 0.8570 nm). In fact, from the neutron powder diffraction on $\text{Ce}_2\text{Pd}_2\text{Sn}$ [19, 20], one can deduce that the first neighbors Ce-Ce spacing is along c axis (Ce1-Ce2=0.4038 nm [7] and Ce3-Ce4=0.5902 nm).

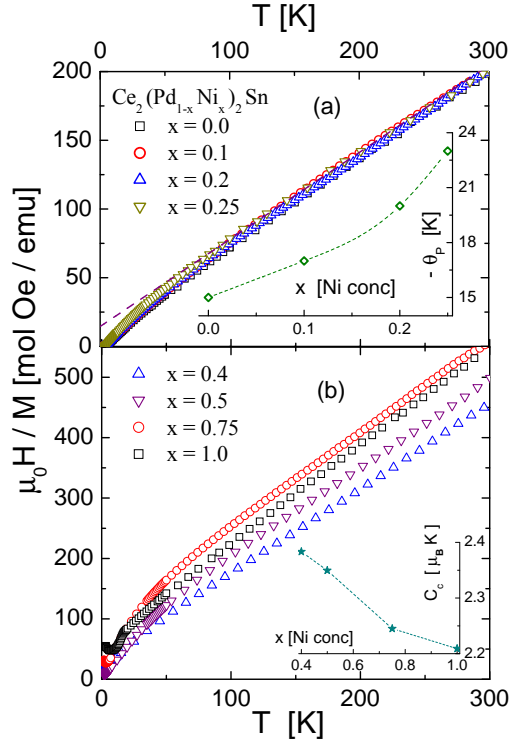


FIG. 2: (Color online) High temperature inverse susceptibility for (a) Pd-rich region and (b) Ni-rich one, measured with $\mu_0 H = 1$ kOe. Respective insets represent the Ni concentration dependencies of (a) Curie-Weiss temperature and (b) Ce effective magnetic moment μ_{eff} on the Ni-rich side.

B. Magnetic Susceptibility

The inverse of the magnetic susceptibility of $\text{Ce}_2(\text{Pd}_{1-x}\text{Ni}_x)_2\text{Sn}$ measured between 1.8 K and room temperature is shown in Figs. 2a and b. On the Pd-rich side a Curie-Weiss behavior $1/\chi = (T + \theta_P)/C_C$ is observed for $T > 100$ K, see dashed line in Fig. 2a. The Curie-Weiss paramagnetic temperature θ_P , extrapolated from $T > 100$ K, slightly decreases from -15 K at $x = 0$ to -23 K at $x = 0.25$, see the inset in Fig. 2. Coincidentally, the computed effective magnetic moments, computed from the Curie constant C_C , are $\mu_{eff} = 2.5 \pm 0.02 \mu_B$, which corresponds to the Ce^{3+} magnetic moment. The negative curvature of $1/\chi(T)$ below 11 K can be attributed to the electric crystal field effect CFE as the excited levels become thermally depopulated.

A different behavior is observed in Fig. 2b for the Ni-rich side. Using the same Curie-Weiss description, increasing values of θ_P from -25 K to -55 ± 5 K are extracted. The Curie constant de-

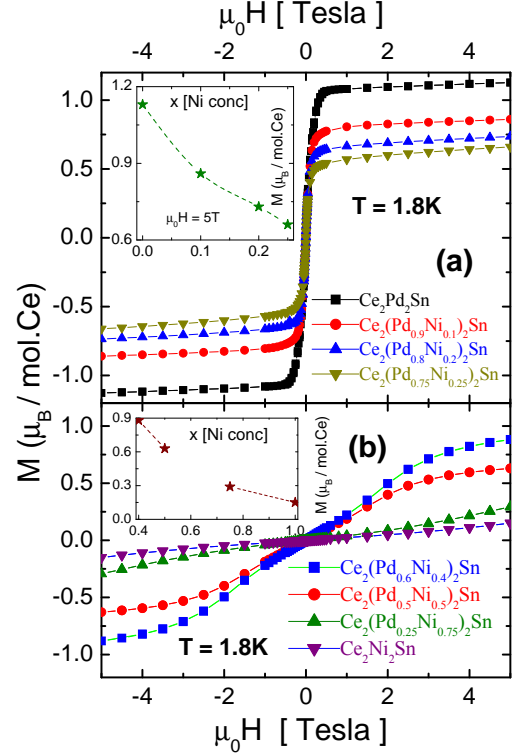


FIG. 3: (Color online) Field dependent magnetization of the 1.8K isotherms, (a) for the Pd-rich region and (b) for the Ni-rich one, measured up to 5 T. Respective insets represent the Ni concentration dependencies of the magnetization values at $\mu_0 H = 5$ T.

creases concomitantly with Ni concentration, from $2.38 \pm 0.02 \mu_B$ for $x = 0.4$ to $2.2 \mu_B$ for $x = 1$, as shown in the inset of Fig. 2b.

The low temperature magnetization was measured at selected temperatures ($T = 1.8, 3, 4$ and 5 K) up to $\mu_0 H = 5$ Tesla. The most relevant information is extracted from the $M(H)$ isotherms measured at $T = 1.8$ K which are displayed in Figs. 3a and b for the respective Pd-rich and Ni-rich sides. On the Pd-rich one, the $M(H)$ dependence shows the typical behavior for a FM phase which saturates around 0.5 T, but with a decreasing moment from $1.13 \mu_B$ for $x = 0$ to $0.66 \mu_B$ for $x = 0.25$. These values were measured at $\mu_0 H = 5$ T and are shown in the inset of Fig. 3a. Despite the expected saturation moment for the free Ce^{3+} ion with total angular momentum $J = 5/2$ according to Hund's rules is $g_J J = 2.14 \mu_B$, the observed value is coherent with a doublet ground state GS with low but increasing hybridization (i.e. Kondo screening) effect. The measured value for the stoichiometric compound $\text{Ce}_2\text{Pd}_2\text{Sn}$ is in agreement with those reported in the literature [14, 20]

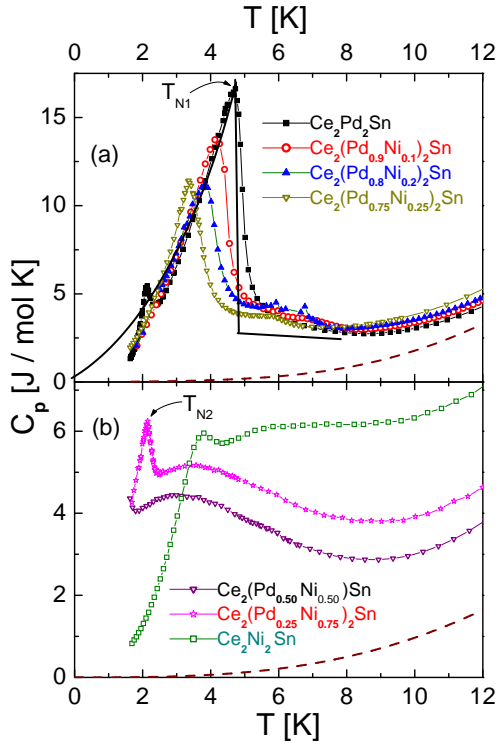


FIG. 4: (Color online) Thermal dependence of specific heat C_P for (a) Pd-rich and (b) Ni-rich phases. Dashed curves represent the respective phonon contributions extracted from La compounds. (a) Continuous curve represents the model calculation from T_K/T_{N1} for $x = 0$, see the text.

Within the Ni-rich phase, the magnetic moment at $\mu_0 H = 5T$ decreases more drastically from $0.9\mu_B$ for $x = 0.4$ to $0.15\mu_B$ for $x = 1$. In Fig. 3b, a qualitative difference in the $M(H)$ dependence can be appreciated between the intermediate Ni concentrated samples and those with Ni concentration $\geq 75\%$, see the inset of Fig. 3b. While $M(H)$ shows a tendency to saturation for $x = 0.4$ and 0.5 , those with $x = 0.75$ and 1.0 still show a positive curvature with significantly lower values of M . This behavior indicates that much larger magnetic field is required to saturate the magnetization approaching the $\text{Ce}_2\text{Ni}_2\text{Sn}$ stoichiometric limit, in agreement with the rapid reduction of the Ce magnetic moment.

C. Specific heat

The low temperature specific heat C_P measurements confirm the magnetic differences between the Ce-GS in both phases. Starting from

$\text{Ce}_2\text{Pd}_2\text{Sn}$ which presents a double magnetic transition [21], the decrease of the AF (upper) one from $T_{N1} = 4.8\text{ K}$ to 3.3 K for $\text{Ce}_2(\text{Pd}_{0.75}\text{Ni}_{0.25})_2\text{Sn}$ can be seen in Fig. 4a. A concomitant decrease of the specific heat jump at $T = T_{N1}$ is observed. On the contrary, the FM (lower) transition at $T_C = 2.2\text{ K}$ for $x = 0$ vanishes upon doping.

The $C_P(T)$ tail above T_{N1} reveals the presence of increasing magnetic correlations related to the formation of magnetic dimers between Ce-next-neighbors [13]. A small hump at around 6 K can be attributed to a little amount of foreign phase, probably $\text{CePd}_{1-x}\text{Ni}_x$, which orders around that temperature [15] or to the contribution of some traces of Ce_2O_3 .

The specific heat of the Ni-rich phase shows a completely different behavior since a weak transition at T_{N2} , which arises with Ni concentration, is followed by a broad maximum, see Fig. 4b. Contrary to the type of transition observed in Fig. 4a, the magnetic transition in $\text{Ce}_2\text{Ni}_2\text{Sn}$ suggests that the ordered phase is formed as a condensation of states which may have itinerant character above T_{N2} . In both 4a and b figures, the phonon references are represented by the respective La compounds, whose contributions are subtracted in order to obtain the magnetic $C_m(T)$ contribution.

IV. DISCUSSION

The temperature dependence of the magnetic susceptibility at high temperature (c.f. $T > 100\text{ K}$) is the characteristic of a Ce system where the six fold levels of the $J = 5/2$ Hund's rule configuration are split by the effect of the electric crystal field CFE. For stoichiometric $\text{Ce}_2\text{Pd}_2\text{Sn}$, the first excited doublet was evaluated at $\Delta_1 \approx 50\text{ K}$ [13]. Such splitting largely exceeds the Kondo temperature and therefore the low temperature magnetic properties on the Pd-rich side can be only attributed to the Kramer's doublet GS. Such is not the case for the Ni-rich phase, where the observed $\theta_P \propto T_K$ temperature is much larger. In this case, the possibility of an overlap between the ground state and the first excited CFE doublet has to be considered because θ_P and Δ_1 become comparable.

The low temperature magnetization curves clearly indicate that in the Pd-rich phase the Ce magnetic moment behaves as strongly localized, whereas on the Ni-rich side it rapidly decreases as the Ni content increases. Noteworthy, the $M(H)$ curve of the $x = 0.4$ sample reaches a relatively high value $\mu = 0.9\mu_B$ at $5T$ for the 1.8 K isotherm. This value is larger than the one of the $x = 0.25$

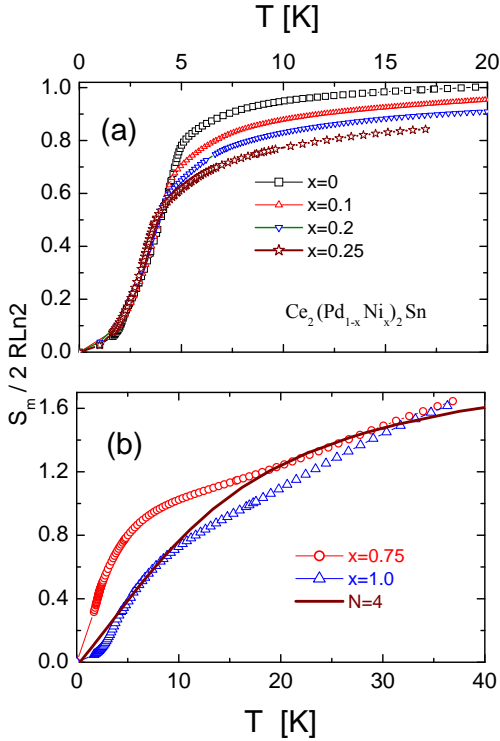


FIG. 5: (Color online) Temperature dependence of the entropy. a) for $x \leq 0.25$ up to $T = 20$ K and b) $x \geq 0.75$ up to $T = 40$ K. Continuous curve: theoretical prediction [28] for a $N=4$ GS with characteristic temperature $T_o = 30$ K.

sample despite its $M(H)$ saturates at quite low applied field $\mu_0 H < 1$ T. This behavior is in line with the localized character of the Ce-4f moment in the Pd-rich phase, whereas on the Ni-rich one it corresponds to an itinerant type of magnetism, which in some Ce compounds may undergo a metamagnetic transition at very high field [22].

A. Pd-rich side

As mentioned before, the thermal variation of C_P for $x < 0.3$ is characterized by a well defined jump ΔC_P at $T = T_{N1}$ which, for $x = 0$, peaks at $\Delta C_P = 8.3$ J/KmolCe instead of $\Delta C_P(T_K = 0) = 12.5$ J/KmolCe, as expected for a $S = 1/2$ two-level system. By increasing Ni concentration, both $\Delta C_P(T_{N1})$ and T_{N1} decrease (see Fig. 4a) which indicates a moderate growing of hybridization effects driving a progressive increase of $T_K(x)$.

In order to evaluate the Kondo temperature $T_K(x)$ variation within this low Ni concentration range, we have applied a resonant level model

based on molecular field calculations for spin 1/2 [21] to describe the ΔC_P as a function of the T_K/T_{N1} ratio. From the $\Delta C_P(x=0)/\Delta C_P(T_K=0)$ ratio a $T_K/T_{N1} = 0.62$ value is obtained for the $x = 0$ sample, see continuous curve in Fig. 4a. This value corresponds to $T_K \approx 3$ K, which rises up to 4.5 K for $x = 0.25$ (not shown). In spite of this increase, it is clear that T_{N1} and T_K energy scales are comparable within this concentration range.

In Fig. 5, we show the thermal evolution of the magnetic entropy computed as $S_m = \int C_m/T dT$. Notice that the entropy is evaluated in 'per Ce-atom' units. The behavior shown by the alloys belonging to the Pd-rich side (see Fig. 6a) is the expected for well localized 4f-moments. The plateau of $S_m(T)$ around $T = 20$ K confirms that the doublet GS is completely occupied at that temperature and that the first excited CFE doublet does not contribute to the magnetic GS properties. By applying the Desgranges-Schotte [23] criterion of $S_{mag}(T = T_K) \simeq 2/3 R \ln 2$ for single Kondo atoms, the extracted values of $T_K(x)$ variation nicely coincide with those extracted from the mentioned analysis of the $\Delta C_P(T_K/T_N)$ jump.

B. Ni-rich side

The peculiar behavior of the specific heat on the Ni-rich side merits a deeper analysis because, as shown in Fig. 4b, a weak transition at $T = T_{N2}$ is followed by a very broad maximum at higher temperature. This unexpected thermal dependence can be explained once the onset of T_{N2} is taken into account. By extrapolating this order temperature to zero, i.e. $T_{N2} \rightarrow 0$ decreasing Ni content as depicted in the phase diagram of Fig. 7, the presence of a Quantum Critical Point QCP [24] can be expected at $x_{cr} = 0.35 \pm 0.05$.

It is well known that the existence of a QCP affects the thermal properties due to the associated low energy quantum fluctuations which induce a peculiar thermal dependencies in the physical parameters known as non-Fermi-liquid behavior [25]. One of the theoretical predictions widely observed experimentally is a $C_m(T)/T \propto -\text{Log}(T/T^*)$ dependence, where T^* is a characteristic energy scale describing the thermal extension of the $C_m(T)/T$ tail. Such a behavior is observed for the $x = 0.5$ and 0.75 samples (with respective $T_{N2} < 1.5$ and $= 2.14$ K) as depicted in Fig. 6. In $\text{Ce}_2\text{Ni}_2\text{Sn}$ that temperature dependence above the transition is practically dominated by classical magnetic correlations because at $T_{N2} = 3.8$ K quantum fluctuations are overcome by classical thermal fluctuations [26]

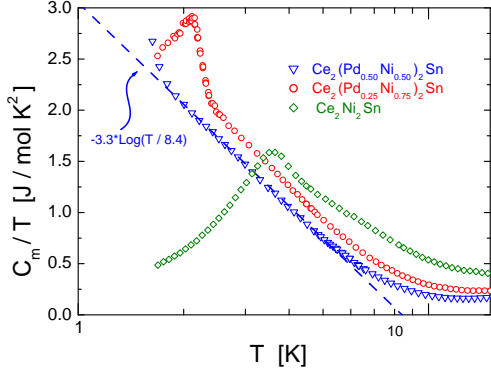


FIG. 6: (Color online) Logarithmic dependence of the magnetic contribution to specific heat divided by temperature for the Ni-rich samples. Dashed line represents the computed logarithmic reference dependence for sample $x = 0.5$.

There is an apparent contradiction within the magnetic behavior observed in these Ni-rich samples. While their $M(2\text{K}, 5\text{T})$ values rapidly decrease with increasing Ni content (see the inset in Fig. 3b), the mentioned weak AF transition temperature and the $\Delta C_m(T_{N2})$ jump increase from $T_{N2} \approx 1.5\text{K}$ up to $T_{N2} \approx 3\text{K}$ at $x = 1$. This complex behavior can be understood by comparing T_K and the splitting of the first excited CFE doublet Δ_1 .

According to $\theta_P(x)$ values within this Ni-rich concentration region, an enhancement of the Kondo screening (i.e. T_K) is expected respect to the tetragonal phase. Within this context, $T_K(x)$ becomes comparable to Δ_1 . Unfortunately, a direct and independent evaluation of these parameters is no possible. However, the analysis of the thermal variation of the magnetic contribution to the entropy provides significant information about the broadened levels distribution.

Since the specific heat of the samples with higher Ni content (i.e. $x = 0.75$ and 1.0) was measured up to 40K , one can trace $S_m(T)$ up to quite high temperature, as it is shown in Fig. 5b. In that figure it can be seen how $S_m(T)$ overcomes the $2R\ln 2$ value already at $T \approx 9\text{K}$ and continuous to grow up to $S_m = 0.8 * (2R\ln 4)$ at $T = 40\text{K}$. Similar behavior is observed in the $x = 1$ sample (i.e. $\text{Ce}_2\text{Ni}_2\text{Sn}$) but with $S(T)$ increasing in a more monotonous manner. Compared with the $S_m(T)$ behavior of a sharp energy distribution of levels, provided by the results depicted in Fig. 5a, it becomes evident an overlap of the side levels of the ground and first excited CFE levels.

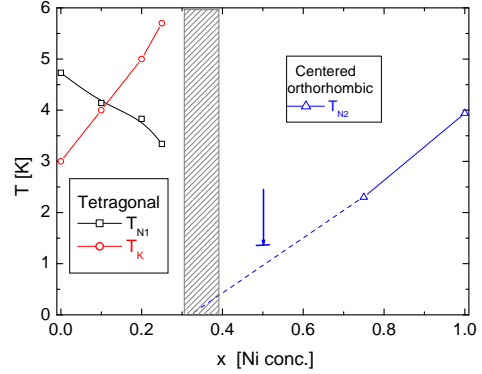


FIG. 7: (Color online) Magnetic phase diagram of the $\text{Ce}_2(\text{Pd}_{1-x}\text{Ni}_x)_2\text{Sn}$ series including both structural phases. The arrow indicates the lower limit of the experimental specific heat measurement for $x = 0.5$ and the dashed line the proposed extrapolation to $T_{N2} = 0$.

This is the key to understand the complex magnetic behavior of this Ni-rich alloys which show a decrease of the magnetic moment with a simultaneous increase of a weak T_{N2} . The former effect is driven by the increase of the $4f$ state hybridization whereas the latter is driven by the increase of the GS density of states due to the arising contribution of the low energy levels of the CFE excited state. Such an enhancement of the low energy density of states is supported by the increasing C_m/T contribution to the specific heat above T_{N2} deduced from Fig. 6, which increases from 0.2J/molK^2 for $x = 0.5$ up to 0.45J/molK^2 for $x=1$ around $T \approx 15\text{K}$. Low effective moments and relatively high ordering temperatures are typical of itinerant magnetic systems [27], provided that the density of states is large enough. This scenario is favored by the reduction of the Ce-Ce spacings decrease driven by the reduction of a and b lattice parameters.

Within a simplified picture, such would be the expected way to undergo from a $N = 2$ degenerated GS to a $N = 4$ degenerated GS in a continuous way. In Fig. 5b we include a theoretical prediction [28] for a $N=4$ degenerated state with a characteristic temperature $T_o = 30\text{K}$. This comparison clearly indicates that, despite of the energy levels contribution of the first excited CFE state, the $N=4$ GS is not reached in this system. Similar situation was observed in other strongly anisotropic Ce systems such as CeTiGe [22].

The low temperature magnetic properties are resumed in the magnetic phase diagram presented in Fig. 7. On the Pd-rich side the comparable magnetic and Kondo energy scales can be appreciated

whereas on the Ni-rich side the extrapolation of $T_{N2} \rightarrow 0$ is evaluated at $x_{cr} = 0.35 \pm 0.05$.

V. CONCLUSIONS

The substitution of Pd atoms by isoelectronic Ni leads to a change in the crystallographic structure from a tetragonal lattice for $x \leq 0.3$ to a centered orthorhombic lattice for $x \geq 0.4$ after about 1% of volume collapse at the structural modification.

The volume contraction in the Pd-rich side induces a moderate increase of the Kondo temperature whose value is comparable to T_{N1} . This induces a decrease of T_{N1} until the limit of this

phase stability. On the Ni-rich side the system behaves as a weakly magnetic heavy fermion with an enhanced degenerate ground state. Notably, an incipient magnetic transition T_{N1} arises in the Ni-rich side favored by the increasing low energy density of states whereas the specific heat shows a $C_m/T \propto -\text{Log}(T/T^*)$ dependence which is the finger print for a quantum critical point extrapolated at $x_{cr} = 0.35$. Lower $C_m(T)$ measurements are required to verify this unexpected behavior occurring in an itinerant magnetic medium. Due to the similar T_K and CFE splitting energy scales, the ground and the first CFE excited states start to overlap without reaching a four fold degenerated GS.

-
- [1] F. Hulliger, *J. Alloys & Comp.* **221** (1995) L11.
 - [2] M. Giovannini, H. Michor, E. Bauer, G. Hilscher, P. Rogl, T. Bonelli, F. Fauth, P. Fischer, T. Hermannsdorfer, L. Keller, W. Sikora, A. Saccone, R. Ferro, *Phys. Rev. B* **61** (2000) 4044.
 - [3] F. Mirambet, P. Gravereau, B. Chevalier, L. Trut. J. Etourneau; *J. Alloys and Comp.* **191** (1993) L1.
 - [4] R.A. Gordon, Y. Ijiri, C.M. Spencer, F.J. DiSalvo, *J. Alloys and Comp.* **224** (1995) 101.
 - [5] D. Kaczrowsky, P. Rogl, K. Hiebl, *Phys. Rev. B* **54** (1996) 9891.
 - [6] M.N. Peron, Y. Kergadallan, J. Rebizant, D. Meyer, S. Zwirner, L. Havela, H. Nakotte, J.C. Sprilet, G.M. Kalvius, E. Colineau, J.L. Oddou, C. Jeandey, J.P. Sanchez, *J. Alloys and Comp.* **201** (1993) 203.
 - [7] F. Fourgeot, P. Gravereau, B. Chevalier, L. Fournès, J. Etourneau, *J. Alloys and Comp.* **238** (1996) 102.
 - [8] E. Bauer, G. Hilscher, H. Michor, Ch. Paul, Y. Aoki, H. Sato, D.T. Adroja, J-G. Park, P. Bonville, C. Godart, J. Sereni, M. Giovannini and A. Saccone, *J. Phys.: Condens Matter* **17** (2005) S999.
 - [9] E. Bauer, R.T. Khan, M. Giovannini, C. Ritter; *Phys. Stat. Sol.* **247** 717 (2010).
 - [10] M. S. Kim, M.C. Bennett and M.C. Aronson; *Phys. Rev. B* **77** 144425 (2008).
 - [11] D. Laffargue, F. Fourgeot, F. Bourée, B. Chevalier, T. Roisnel and J. Etourneau, *Solid State Commun.* **100** 575 (1996).
 - [12] S. Miyahara and K. Ueda; *Phys. Rev. Lett.* **82** 3701 (1999).
 - [13] J.G. Sereni, M. G.- Berisso, A. Breghta, G. Schmerber and J.P. Kappler, *Phys. Rev. B* **80** 024428 (2009).
 - [14] J.G. Sereni, M. Gomez Berisso, A. Braghta, G. Schmerber and J.P. Kappler, *Phys. Rev. B* **81** 184429 (2010).
 - [15] J.P. Kappler, G. Schmerber, J.G. Sereni; *J. Magn. Magn. Materials* **76 & 77** (1988) 185.
 - [16] F.J. DiSalvo, R.A. Gordon, C.M. Spencer, Y. Ijiri; *J. Alloys and Compd.* **224** (1995) 101.
 - [17] F. Fourgeot, B. Chevalier, P. Gravereau, L. Fournès, J. Etourneau, *J. Alloys and Compd.* **218** (1995) 90.
 - [18] Y. Ijiri and F.J. DiSalvo; *J. Alloys and Compd.* **233** (1996) 69.
 - [19] D. Laffargue, S. Bordère, F. Bourée, B. Chevalier, J. Etourneau, T. Roisnel, *J. Phys.: Condens Matter* **11** (1999) 5195.
 - [20] D. Laffargue, F. Bourée, B. Chevalier, J. Etourneau, T. Roisnel; *Physica B* **259-261** (1999) 46.
 - [21] A. Braghta, G. Schmerber, A. Derory, J.G. Sereni, J.P. Kappler, *J. Magn. and Magn. Materials* **320** (2008) 1141.
 - [22] See e.g. M. Deppe, N. Caroca-Canales, J.G. Sereni, C. Geibel; *J. of Phys. Conf. Series* **200** 012026 (2009).
 - [23] H.-U. Desgranges and K.D. Schotte, *Physics Letters* **91A** 240 (1982).
 - [24] H.v. Löhneysen, A. Rosch, M. Vojta, P. Wölfle, *Rew. Mod. Phys.* **79** (2007) 1015.
 - [25] G.R. Stewart; *Rew. Mod. Phys.* **73** 797 (2001).
 - [26] J.G. Sereni; *J. Low Temp. Phys.* **147** 179 (2007).
 - [27] L.E. DeLong; *J. Magn. Magn. Mat.* **62** (1986) 1.
 - [28] B. Coqblin and J.R. Schrieffer, *Phys. Rev.* **185** 847 (1969).